Physical Chemistry Chemical Physics c3cp55358b

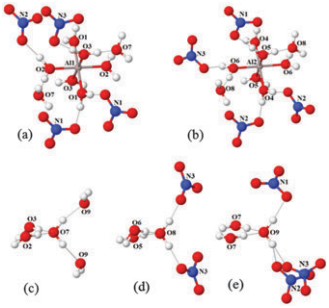

Large polarization but small electron transfer for water around Al^{3+} in a highly hydrated crystal Q1 Q2

Pavlin D. Mitev, Imre Bakó, Anders Eriksson and Kersti Hermansson*

Precise molecular-level information on the water molecule is precious, since it affects our interpretation of the role of water in a range of important applications of aqueous media. Q4

Please check this proof carefully. **Our staff will not read it in detail after you have returned it.**

Translation errors between word-processor files and typesetting systems can occur so the whole proof needs to be read. Please pay particular attention to: tabulated material; equations; numerical data; figures and graphics; and references. If you have not already indicated the corresponding author(s) please mark their name(s) with an asterisk. Please e-mail a list of corrections or the PDF with electronic notes attached – do not change the text within the PDF file or send a revised manuscript. Corrections at this stage should be minor and not involve extensive changes. All corrections must be sent at the same time.

Please bear in mind that minor layout improvements, e.g. in line breaking, table widths and graphic placement, are routinely applied to the final version.

Please note that, in the typefaces we use, an italic vee looks like this: ν, and a Greek nu looks like this: ν.

We will publish articles on the web as soon as possible after receiving your corrections; **no late corrections will be made.**

Please return your **final** corrections, where possible within **48 hours** of receipt, by e-mail to: pccp@rsc.org

Queries for the attention of the authors

Journal: **PCCP**

Paper: **c3cp55358b**

Title: **Large polarization but small electron transfer for water around Al^{3+} in a highly hydrated crystal**

Editor's queries are marked on your proof like this Q1, Q2, etc. and for your convenience line numbers are indicated like this 5, 10, 15, ...

Please ensure that all queries are answered when returning your proof corrections so that publication of your article is not delayed.

Query reference	Query	Remarks
Q1	For your information: You can cite this article before you receive notification of the page numbers by using the following format: (authors), Phys. Chem. Chem. Phys., (year), DOI: 10.1039/c3cp55358b.	
Q2	Please carefully check the spelling of all author names. This is important for the correct indexing and future citation of your article. No late corrections can be made.	
Q3	Although there is a discussion of ESI in the text, ESI does not appear to have been provided. Do you wish to provide ESI or would you like this citation to be removed or changed?	
Q4	Please check that the inserted GA image and text are suitable.	
Q5	Please check that ref. 17 and 22 have been displayed correctly.	

PCCP

PAPER

Large polarization but small electron transfer for water around Al^{3+} in a highly hydrated crystal†

Cite this: DOI: 10.1039/c3cp55358b

Pavlin D. Mitev,[a] Imre Bakó,[ab] Anders Eriksson[a] and Kersti Hermansson*[a]

Received 20th December 2013,
Accepted 13th March 2014

DOI: 10.1039/c3cp55358b

www.rsc.org/pccp

Precise molecular-level information on the water molecule is precious, since it affects our interpretation of the role of water in a range of important applications of aqueous media. Here we propose that electronic structure calculations for highly hydrated crystals yield such information. Properties of nine structurally different water molecules (19 independent O···O hydrogen bonds) in the $Al(NO_3)_3{\cdot}9H_2O$ crystal have been calculated from DFT calculations. We combine the advantage of studying different water environments using one and the same compound and method (instead of comparing a set of independent experiments, each with its own set of errors) with the advantage of knowing the exact atomic positions, and the advantage of calculating properties that are difficult to extract from experiment. We find very large Wannier dipole moments for H_2O molecules surrounding the cations: 4.0–4.3 D (compared to our calculated values of 3.1 D in liquid water and 1.83 D in the gas phase). These are induced by the ions and the H-bonds, while other water interactions and the relaxation of the internal water geometry in fact *decrease* the dipole moments. We find a good correlation between the water dipole moment and the O···O distances, and an even better (non-linear) correlation with the average electric field over the molecule. Literature simulation data for ionic aqueous solutions fit quite well with our crystalline 'dipole moment *vs.* O···O distance' curve. The progression of the water and cation charges from '*small clusters* ⇒ *large clusters* ⇒ *the crystal*' helps explain why the net charges on all the water molecules are so small in the crystal.

1. Introduction

The influence of an ion on its surrounding hydration shell in aqueous media keeps intriguing the scientific community, since the phenomenon is both complicated from a fundamental point of view, and has far-reaching practical consequences. The crucial role of water in mineralogy, biology, electrochemistry and materials science (think gypsum, for example, or corrosion) is to a large extent governed by the ion–water interactions and how they affect the water molecule's H-bonding ability, stability, acidity and mobility. One of the most significant effects of a cation on a neighbouring water molecule is the increase of the molecule's dipole moment. Compared to the gas-phase water dipole moment (experimental value 1.85 D)[1] the increase is large, but whether it is larger than the average dipole moment of, say, liquid water or ice depends on the ion.

For ion–water systems, there exist several quantum-mechanical studies in the literature where the dipole moment of water in small gas-phase clusters and chains has been reported; a fairly recent example is the study of K^+(aq) and Ca^{2+}(aq) clusters by Bucher and Kuyucak in 2008.[2] There also exist a number of theoretical studies reporting water dipole moments for ionic aqueous solution. Typically these originate from *ab initio* molecular dynamics simulations, such as Car–Parrinello molecular dynamics (CPMD) simulations.[2–14]

We are not aware of any report of the water dipole moment in *hydrates of ionic crystals* in the literature. The crystalline state has certain advantages over the liquid state when it comes to providing firm information about structure–property relationships and bonding correlations: more precise structural information is often available and easier to define. This paper discusses the crystalline hydrate $Al(NO_3)_3{\cdot}9H_2O$, where the water molecules are crystallographically independent so that there are 9 water molecules, with 18 H atoms, which all have different surroundings. Six of the water molecules reside in the first hydration shell of the (nominal) Al^{3+} ions, two in the second shell and one in the third, although the classification of the second and third shells becomes somewhat dubious in a crystal.

The $Al(NO_3)_3{\cdot}9H_2O$ structure thus opens up a rather unusual possibility to study water molecules and hydrogen bonds of

[a] Department of Chemistry, The Ångström Laboratory, Uppsala University, Box 538, S-751 21 Uppsala, Sweden. E-mail: kersti@kemi.uu.se
[b] Institute of Structural Chemistry, Chemical Research Center of the Hungarian Academy of Sciences, Pusztaszeri út 59-67, H-1025 Budapest, Hungary

† Electronic supplementary information (ESI) available: Tables S1–S3 showing calculated and experimental interatomic distances and angles and Table S4 showing calculated charges. See DOI: 10.1039/c3cp55358b

different types within one and the same crystal. This reduces the effect of systematic errors, as one and the same experiment or calculation can yield information that would otherwise require a set of independent experiments/calculations, each with its own set of errors. Here we make use of this advantage and monitor how the polarization of a water molecule varies with its environment. The eighteen different H-bonds in $Al(NO_3)_3{\cdot}9H_2O$ span a large O···O distance range: between 2.65 and 2.85 Å, as measured from the neutron diffraction study of the deuterated compound.[15]

The first goal of this paper is to find out whether key properties related to molecular polarization – such as the induced dipole moment itself, the "external" electric field over the water molecules, and the electron redistribution caused by the environment – are indeed sensitive structural probes and manage to reflect the structural differences between the nine water molecules in the crystal. (The answer is yes, and two main groups emerge.) *The second goal* is to find out how much polarized a water molecule can become in such a highly polarizing crystalline surrounding as we have in $Al(NO_3)_3{\cdot}9H_2O$. (The answer is: a lot.) *The third goal* is to find out whether the ion–water interactions, the water network and the distortion of the internal water geometry all contribute to the enhancement of the water dipole moments. (The answer is no.) *The fourth goal* is to make use of this rather unusual compound with its 18 independent O–H bonds to explore some interesting *hydrogen-bond* correlations. (It is useful. Traditional H-bond correlations are fulfilled and we also discover a new one: a 'water dipole moment *vs.* H···O distance' correlation with a slope of about −6.0 Debye $Å^{-1}$).

For all this we will use quantum-mechanical density functional theory (DFT) to first optimize the crystal structure of $Al(NO_3)_3{\cdot}9H_2O$ and then calculate dipole moments of the Wannier and Bader types (see the Method part) and the other properties mentioned.

2. Method and models

2.1 General

Electronic spin-unpolarized calculations for $Al(NO_3)_3{\cdot}9H_2O$ were performed within the framework of periodic plane-wave density functional theory (DFT) calculations. All energy and electron density calculations were performed using the Perdew–Burke–Ernzerhof (PBE)[16] form of GGA. Long-range van der Waals forces were included by using the DFT-D2 approach.[17] The electrons kept in the core region were $1s^2 2s^2 2p^6$ for Al, $1s^2$ for N and O; these were described by PAW potentials.[18] The plane-wave cutoff was 800 eV, and a 5 × 5 × 5 Monkhorst–Pack grid[19] of *k*-points was used to sample the Brillouin zone. All wavefunction calculations for the crystal were performed using the VASP program.[20,21]

2.2 Structure model and optimization

The $Al(NO_3)_3{\cdot}9H_2O$ crystal structure determined from diffraction is monoclinic with space group $P2_1/c$ (see ref. 15 and references therein). The crystal structure was optimized starting from the experimental structure in ref. 15, but the symmetries of the space group were not imposed. Thus, all cell parameters and all atomic coordinates were optimized until all forces on all atoms were smaller than 0.010 eV $Å^{-1}$. In the results and discussion section we first establish whether our DFT calculations reproduce the experimental structure from neutron diffraction faithfully enough to allow us to make strong connections between our model crystal and the real crystal. This is the case, and we also note that the energy minimum found yields α and γ angles extremely close to 90° and preserves the symmetry elements of the $P2_1/c$ space group. This is the structure we have chosen to work with.

2.3 Bader charge and dipole moment calculations

Atomic charges were obtained from the VASP-calculated electron density using the *atoms in molecules* theory of Bader[22,23] as implemented in the program of Henkelman *et al.*[24] The valence electron density was analyzed for atomic basins that were determined from the total electron density (a core contribution is added).

The electric dipole moments were calculated from the local dipole moments within the three atomic basins for each water molecule, plus the contributions from the net charge (nucleus + electrons) within each basin. The water molecules are all close to neutral (magnitude less than 0.05 *e*; see Table 5), but not exactly so and thus the resulting dipole moment is origin-dependent. It is therefore important to choose the origin in a consistent manner when features of different water molecules are compared. Here we used the O nucleus as the origin. Choosing the midpoint between the two H nuclei as the origin (an extreme shift) would change the dipole moments systematically for all molecules, and by less than 0.2 D.

We also made a systematic investigation of the convergence of the charges and dipole moments with respect to the number of grid-points used in the program by Henkelman *et al.*[24] We finally used a mesh of 800 × 600 × 650 points along the cell axes, corresponding to 0.017 Å between grid-points. This is perhaps an unnecessarily fine grid, since we found that using a slightly coarser grid (600 × 450 × 500 points; 0.022 Å between points) changed the Bader atomic charges by less than 0.007 *e* and using an even coarser grid (400 × 270 × 300 grid; 0.035 Å between points) led to charges that differed by less than 0.016 *e* from the charges obtained from the very fine grid used in this paper.

2.4 Dipole moment calculations from Wannier centers

Wannier orbitals and their centers[25] were calculated from the final electronic wave function using the WANNIER90 program.[26] From the positions of these centers and the atomic nuclei the dipole moment of each water molecule was calculated.

2.5 Electron difference density maps

The difference electron density, $\Delta\rho = \rho(\text{crystal}) - [\Sigma\rho(H_2O) + \Sigma\rho(NO_3^-) + \Sigma\rho(Al^{3+})]$, where the sum is over all ions and water molecules in the crystal. $\Delta\rho$ displays the electron *re*distribution

caused by *inter*molecular interaction in the crystal. In this calculation, the crystal "molecular" fragments subtracted (the isolated water molecules, the isolated nitrate ions and the isolated Al^{3+} ions) were all fixed at the geometry of the optimized crystal.

2.6 Electric field calculations

Electric field calculations were performed and will be discussed in the Results section.

2.7 Reference calculations for the isolated water molecule

Reference calculations using the VASP program were performed for two types of isolated water molecules: (i) for the geometry-optimized free water molecule, and (ii) for the nine water molecules "taken out from" the crystal and kept fixed at the geometry of the crystal. The latter were used for the calculations of the difference electron density maps discussed in Section 3.3. In all cases, the water molecule (with its crystal geometry) was placed in a periodic cubic box with dimensions 12.43 × 12.43 × 12.43 Å^3, and only the gamma point was used for the *k*-point grid. All other settings were the same as for the crystal calculations.

Our optimized geometry of the free water molecule at the PBE-D2 level is 0.972 Å for the OH distance and 104.4° for the angle. The dipole moment calculated from integration in the VASP program is 1.825 D. This value should be the same as those obtained from the Bader and Wannier methods, which it is; all three agree within 0.003 D.

2.8 Cluster calculations using Gaussian

Calculations for isolated clusters (cluster fragments taken out of the crystal) were performed for the purpose of examining how the net atomic and molecular charges develop as one goes from small to increasingly large clusters. Here the PBE functional and the 6-311G** basis set[27] were used as implemented in Gaussian-09 program.[28] These calculations will only be discussed in Section 3.5.

3. Results and discussion

3.1 Description of the structure

The dimension of the calculated crystallographic cell is given in Table 1. The agreement with the room-temperature X-ray diffraction-determined cell[15,29] is quite good. The environment around each water molecule and the atomic labels we use are shown in Fig. 1. We follow the atomic labeling scheme of ref. 15. Tables S1–S3 (ESI†) list a selection of bond distances and angles. Fig. 2 shows the agreement between the experimental distances from neutron diffraction[15] and the distances from the present calculation. The H···O and O···O distances agree well, also on an absolute scale. All intramolecular distances (N–O, Al–O and O–H) are about 0.02 Å longer in the calculations compared to experiment but the correlation between experiment and calculation is good. The O9–H91 bond is an outlier in Fig. 2b. This is the only OH bond that is involved in a bifurcated hydrogen bond, *i.e.* one H has two H-bond acceptors, namely O(9)–H(91)···O(23) and O(9)–H(91)···O(33).

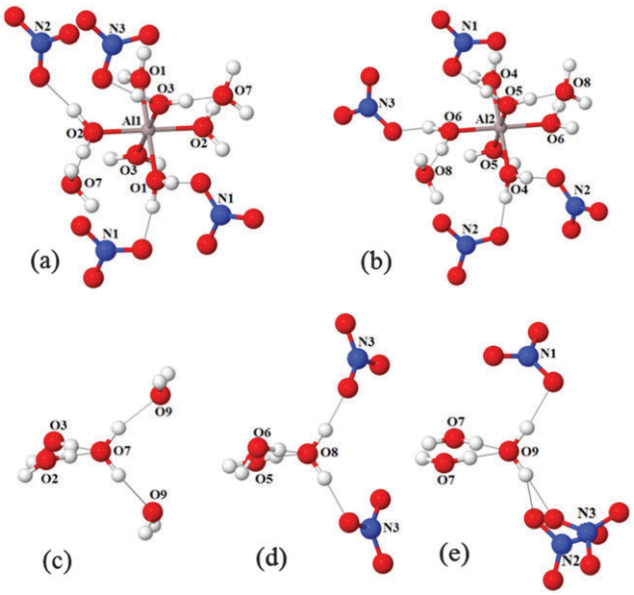

Fig. 1 Selected parts of the calculated crystal structure of $Al(NO_3)_3{\cdot}9H_2O$. The atomic labels are according to the neutron diffraction work by Hermansson.[15] (a) Coordination around Al1 including the hydrogen bond network around W1, W2 and W3. (b) Coordination around Al2 including the hydrogen bond network around W4, W5 and W6. (c–e) The hydrogen bond network around W7, W8 and W9, respectively. Included in ref. 15 are several figures that give more detailed structural information.

Table 1 Resulting cell parameters for the $Al(NO_3)_3{\cdot}9H_2O$ crystal from our DFT calculations compared with diffraction data for $Al(NO_3)_3{\cdot}9D_2O$ from ref. 15 and for $Al(NO_3)_3{\cdot}9H_2O$ from ref. 29. Values within parentheses are standard deviations

	Calc.	Exp. ~300 K $Al(NO_3)_3{\cdot}9D_2O$[15]	Exp. ~300 K $Al(NO_3)_3{\cdot}9H_2O$[29]
a (Å)	13.9733	13.8937 (13)	13.892 (2)
b (Å)	9.4631	9.6258 (7)	9.607 (1)
c (Å)	10.8163	10.9127 (7)	10.907 (2)
β (°)	96.177	95.66 (1)	95.51 (2)
V (Å^3)	1421.9	1452.3 (2)	1448.9

In the literature, there are many reports on correlations involving experimentally determined distances and angles related to hydrogen-bond networks in crystals (see, for example, the rather recent ref. 30 and numerous references therein). The results from the neutron diffraction study of $Al(NO_3)_3{\cdot}9D_2O$[15] show "normal behaviour", *i.e.* they fit very well into the existing correlations.

3.2 O–H distances

We will discuss the O–H distances in some detail. Such a discussion can easily become a little complicated because not only do we want to compare the distances in the solid state with the gas-phase reference (*i.e.*, the effect of the crystalline environment) but in comparison between calculations and experiment we also need to consider equilibrium (r_e) distances

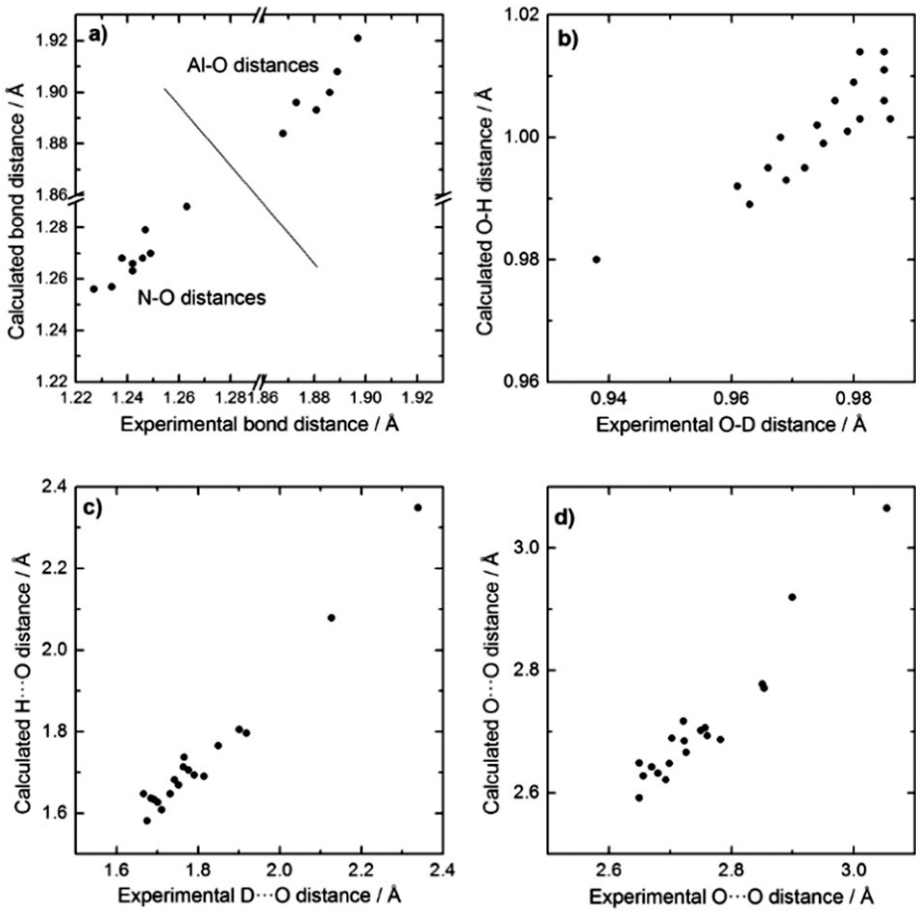

Fig. 2 Calculated equilibrium distances (r_e, this work) *vs.* experimental[15] bond distances. (a) N–O and Al–O distances. (b) O–H (O–D) distances. Note that the horizontal and vertical scales are different. (c) Hydrogen bond H···O (D···O) distances. (d) Hydrogen bond O···O distances.

versus vibrationally averaged distances (r_0), and O–H distances *versus* O–D.

Optimization of the gas-phase water structure using the same DFT method as we use for the crystal yields the equilibrium O–H distance, r_e(O–H), of 0.972 Å and a water angle of 104.4°. This is about 0.015 Å longer than the experimental equilibrium distance (0.9572 Å),[31] which could explain part of the systematic deviation between the experimental and calculated absolute O–H distances seen in Fig. 2b and Fig. 3.

We note that in the calculations, the r_e(O–H) distances for the nine water molecules in the crystal are all *longer* than the gas-phase value of 0.972 Å (0.01–0.04 Å longer according to Table S2, ESI†). The gas-phase reference state is marked by the line labeled "r_e(O–H) for H_2O(g)" in Fig. 2b. It should be noted, however, that the label could equally well be denoted "r_e(O–D) for D_2O(g)", as the r_e value is independent of the isotopic substitution. For the experiments, the appropriate gas-phase value to compare with is the mean O–D distance of a gas-phase D_2O molecule in the vibrational ground state (0.9687 Å),[31] marked "r_0(O–D) for D_2O(g)" in Fig. 2a. The experimental room-temperature diffraction-determined O–D distances for the deuterated crystal in ref. 15 lie in the range 0.938–0.986 Å and *surrounding* the experimental gas-phase value. The experiments thus suggest that the intramolecular water distances are either shortened or elongated by the crystal surroundings. There is clearly a qualitative discrepancy between experiment and calculations here, which we will discuss a little more.

It is difficult to determine equilibrium O–H (or O–D) distances for crystalline water accurately from neutron diffraction. This is so *both* because the neutron diffraction refinement yields the distances between mean nuclear positions (and not mean distances), *and* because appropriate models of vibrational anharmonicity and of librational curvilinear motion are rather difficult to include properly in the experimental refinement procedure. This easily leads to systematic errors of the order of 0.01–0.02 Å[32,33] for neutron diffraction-determined water O–H (or O–D) distances, even though the published standard deviations from the least-squares structure refinement procedure are usually much smaller. The experimental neutron-diffraction-determined O–D distances in the $Al(NO_3)_3 \cdot 9D_2O$ crystal are obviously *systematically erroneous and too short* since the surroundings should always lengthen the O–H (or O–D) bonds in a water molecule compared to the gas-phase value. This is indeed what the calculations give, and the calculations can thus provide valuable complementary information

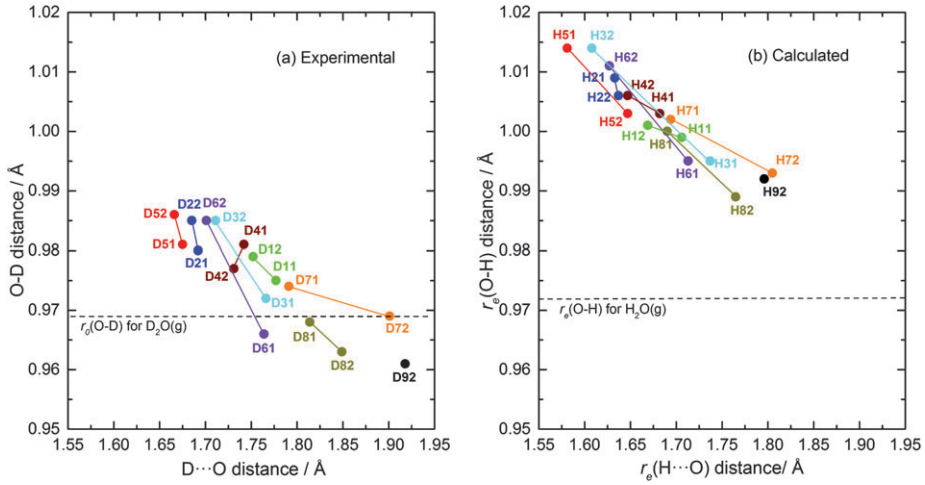

Fig. 3 O–H (O–D) bond distances in water molecules *vs.* corresponding H···O (D···O) hydrogen bond distances. The two bonds of the water molecules are represented by a certain color code for the two hydrogen atoms involved. H91 is not included because of its participation in a bifurcated hydrogen bond. The dashed lines are the gas-phase reference values for unbound water molecules (see text). (a) From neutron diffraction on $Al(NO_3)_3 \cdot 9D_2O$(s).[15] The r_0(O–D) distance is for the ground vibrational state. (b) From calculations on $Al(NO_3)_3 \cdot 9H_2O$(s). The r_e distances are equilibrium distances.

about the change of the internal O–H distance due to the surrounding crystal.

As for the issue of the effect of isotopic substitution (O–H *vs.* O–D distances), one can note that, for a specific compound, an experimental O–D distance is normally expected to be shorter than the corresponding O–H distance. One reason is that the O–D vibrational energy levels lie lower than the O–H levels in the anharmonic stretching potential. The r_0(O–H) − r_0(O–D) difference is 0.004 Å for the free water molecule as measured by microwave spectroscopy at room temperature.[31] For bound water molecules, this difference should increase due to increasing anharmonicity. (Incidentally, a value of 0.03 Å has been reported for the water molecule in liquid water, from a combined X-ray and neutron diffraction analysis.[34]) However, as we have pointed out above, in our calculations the distances are r_e values and the issue of O–H *vs.* O–D is irrelevant.

Table 2 Magnitudes of the dipole moments for the water molecules in $Al(NO_3)_3 \cdot 9H_2O$ from Wannier and Bader analyses of the DFT-calculated wavefunction. In all cases, the dipole moment vectors deviate by less than 3° from the water bisector. The dipole moments were calculated using the optimized structure, and are compared with those using the experimentally determined structure from ref. 15 (in parentheses). The calculated dipole moment of the isolated optimized water molecule (0.972 Å and 104.5°) is 1.825(3) D (uncertainty depending on the integration methods)

Water #	Coord. no. (# of Al^{3+}, NO_3^-, H_2O)	Dipole moment (D) from Wannier analysis	Dipole moment (D) from Bader analysis
W1	1 + 2 + 0	3.91 (3.86)	2.99 (2.94)
W2	1 + 1 + 1	4.24 (4.16)	3.26 (3.19)
W3	1 + 1 + 1	3.99 (3.90)	3.01 (2.95)
W4	1 + 2 + 0	4.02 (3.97)	3.06 (3.00)
W5	1 + 1 + 1	4.27 (4.19)	3.26 (3.20)
W6	1 + 1 + 1	4.07 (3.99)	3.17 (3.10)
W7	0 + 0 + 4	3.60 (3.34)	2.64 (2.53)
W8	0 + 2 + 2	3.51 (3.26)	2.54 (21.44)
W9	0 + 3 + 2	3.27 (3.02)	2.50 (2.40)

3.3 Dipole moments

Two groups of water molecules. We have analyzed the dipole moments of the nine water molecules in the $Al(NO_3)_3 \cdot 9H_2O$ crystal, using both the Wannier function formalism and an integration over Bader volumes (Table 2 and Fig. 4). The six water molecules coordinated to Al^{3+} have very large dipole moments, higher than the other three. The magnitudes of the Wannier dipole moments are 3.9–4.3 D and 3.3–3.6 D, respectively, and the direction of the dipole moment vector deviates by less than 3° from the water bisector in all cases. The very high values for the 1st shell water molecules (W1,..., W6) can be seen as the result of a cooperative effect where the strong polarization exerted by the small and highly charged Al^{3+} ion is enhanced by the H-bonds (to nitrate ions and/or water molecules) donated on the other side of the water molecule. Such 'cation − water···H-bond acceptor' arrangements are ideal for dipole enhancement.

W7 is only surrounded by water molecules and is structurally the most bulky of all the water molecules in $Al(NO_3)_3 \cdot 9H_2O$. It is the second-shell to Al^{3+}. W8 is the second-shell to Al^{3+} and also H-bonded to NO_3^-. The dipole moments of these two water molecules are still quite large, 3.5–3.6 D.

W9 is by far the most weakly bound water molecule, or at least the least affected by its surroundings. It is third-shell to Al^{3+} and binds to three NO_3^- ions (two *via* bifurcated H-bonding). The dipole moment is 3.3 D, *i.e.* it is still more polarized than a typical water molecule in bulk liquid water (3.1 D in our simulations using the same functional).

A comparison of the calculated dipole moments based on the DFT-optimized atomic positions (the first entries in the third and fourth columns in Table 2), with the calculated dipole moments based on the experimentally refined atomic positions (the second entries, in parentheses, in the third and fourth columns in Table 2) displays differences of less than 0.26 D for

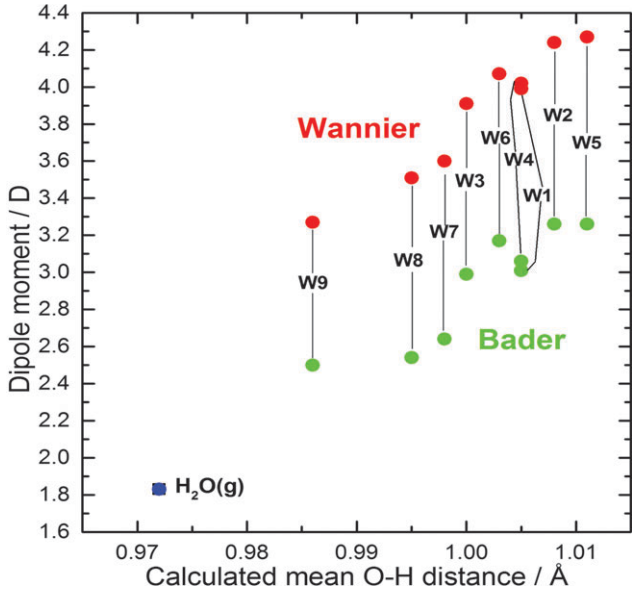

Fig. 4 Calculated Wannier and Bader dipole moments *vs.* the mean value of the O–H bond lengths for each of the nine water molecules. The free water molecule, for which the Wannier and Bader dipole moments have the same value, is also included.

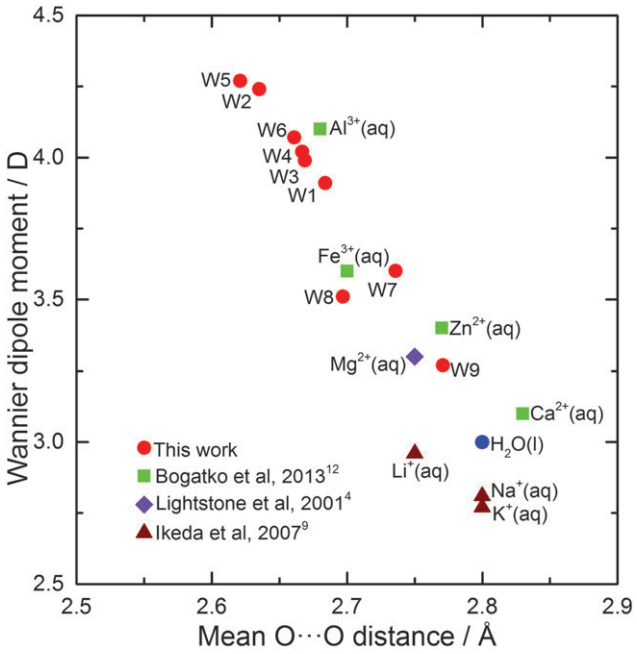

Fig. 5 Some selected calculated dipole moments of water molecules coordinated to metal cations in a crystal (this work) or in aqueous solution plotted *vs.* the mean of the O···O distances (for the aqueous solutions between the first and second hydration shells) as a measure of hydrogen bond strength. W9 is represented only by its non-bifurcated O···O bond.

any water molecule. This confirms that any structural discrepancies between experiment and calculation (due to systematic or random errors) have only a modest influence on the calculated dipole moments.

The water dipole moments in this paper were calculated for the equilibrium geometries (r_e) while experimental geometries for the $Al(NO_3)_3{\cdot}9D_2O$ crystal (in principle) refer to the vibrational ground state at room temperature (r_0) (see the discussion in Section 3.2 above). The difference in the O–D bond length between these two states is about 0.010 Å for the free D_2O water molecule.[31] However, as intermolecular bonding generally increases the anharmonicity of the intramolecular water bond, we believe that the difference ($r_0 - r_e$) will increase when the water is bound. As a test, we have calculated the Wannier dipole moments with an elongation of 0.015 Å for the O–H distances of the water molecules in our $Al(NO_3)_3{\cdot}9D_2O$ crystal (note that our calculations do not make a difference between $Al(NO_3)_3{\cdot}9D_2O$ and $Al(NO_3)_3{\cdot}9H_2O$ as it is r_e that we calculate). The dipole moment then increased by 0.03–0.09 D.

Bader *vs.* Wannier results. Fig. 4 also demonstrates that our dipole moment values obtained from the Bader analysis are 0.8–1.0 D smaller than the corresponding values from the Wannier analysis and that there is a good correlation between the two methods. Dyer and Cummings[35] also obtained a discrepancy when using the two methods to analyze water molecules in H_2O(l); they report a difference of around 0.5 D with the Wannier values larger than Bader values (using the BLYP functional and other pseudopotentials than ours). With the DFT method used in the present paper, PBE-D2, we find that the Wannier and Bader dipole moments from a liquid water simulation differ by about 0.8 D. For the isolated water molecule, the Wannier and Bader partitioning indeed give the same value, namely 1.825(3) D.

A new H-bond correlation for water: dipole moment *vs.* H-bond distance. Theoretical calculations allow us to single out and pinpoint the properties of specific molecules among the rest in a crystal or a liquid. The magnitude of the dipole moment of each water molecule in the $Al(NO_3)_3{\cdot}9H_2O$ crystal is plotted against the mean value of the O···O distances associated with its donated hydrogen bonds in Fig. 5. The nine water molecules are seen to display a good correlation: the shorter the donated H-bond, the larger the dipole moment. The slope is about -6.0 Debye $Å^{-1}$.

Some results from the literature are included in Fig. 5, all concerning the first hydration shell of cations in aqueous solution. In the cited papers, the dipole moment values were always obtained from a Wannier center analysis calculated from the electronic wavefunction for selected snapshots from CPMD simulations using the PBE or BLYP functionals. Thus, Bogatko *et al.*[12] calculated an average value of 3.1 D for the first hydration shell around Ca^{2+}(aq), 3.4 D for Zn^{2+}(aq), 3.6 D for Fe^{3+}(aq), and 4.1 D for Al^{3+}(aq). Four or five snapshots were selected for the dipole moment calculation in each case and the authors gave an error of about ±0.3 D for their water dipole moment and about ±0.08 Å for their O···O distances. Lightstone *et al.*[4] calculated an average dipole moment of 3.3 D for the hydration shell in Mg^{2+}(aq) based on fifteen configurations. For monovalent ions, Ikeda *et al.*[9] reported 3.0 D, 2.8 D and 2.8 D for Li^+(aq), Na^+(aq) and K^+(aq), respectively. Here we have estimated mean O···O distances of 2.75, 2.80 and 2.80 Å (with an uncertainty of ~0.05 Å), respectively, from their radial distribution graphs of the O···O distances. Whitfield *et al.*[14]

also found a value of 2.8 D for K^+(aq). There exist some additional papers in the literature where dipole moments for first-shell water molecules around cations have been calculated, but they have not been included in our graph since the O···O distances between the first and second hydration shells were not reported or they were not easily calculated (by us) from the published data.

Despite the sometimes modest number of snapshots used in the dipole moment analysis for the aqueous solutions in Fig. 5, and the differences in the details of the computational procedures employed, they all seem to approximately fit one and the same 'dipole moment *vs.* H-bond' relation, and moreover, this relation nicely coincides with that followed by our crystalline hydrate.

Relative roles of ions and water molecules in the polarization. Some water–water interactions in the crystal counteract the polarization. Table 3 lists the water dipole moments in a hypothetical crystal where all the ions (Al^{3+} and NO_3^-) have been removed from the optimized $Al(NO_3)_3{\cdot}9H_2O$ structure. In Table 3, W1,..., W6 all have dipole moments smaller than that of the gas-phase molecule. The particularly small dipole moments for W1 and W4 in the hypothetical ion-free crystal tell us that the large induced dipole moments for these molecules in the full crystal (Table 2) are *entirely due to the ions*. The W1,..., W6 molecules occupy octahedral positions around Al^{3+} (now removed in the hypothetical structure) and the interaction among these water molecules is repulsive. A comparison of Tables 2 and 3 shows that for W2, W3, W5 and W6 also, it is the ions, and not the water molecules, that are responsible for the large water dipole moments in the full crystal (Table 2). W2, W3, W5 and W6 are involved in one (attractive and polarizing) hydrogen-bond each, and the net effect from the surrounding water network on these four water molecules is still a dipole moment decrease, but less drastic than for W1 and W4.

W7 is surrounded by four H-bonded water molecules. Comparing Tables 2 and 3 for W7 tells us that the enhancement in the full crystal is *almost entirely due to these water neighbours*. For W8 and W9, the *water neighbors and the ions appear to play approximately equal roles*.

Table 3 Calculation of the contribution of the water-framework-only to the water dipole moments in $Al(NO_3)_3{\cdot}9H_2O$. The table lists the Wannier dipole moments from a single-point calculation for a hypothetical crystal structure where all four cations and twelve anions in the unit cell have been removed, leaving only the entire water framework. The atoms are kept at the positions of the calculated $Al(NO_3)_3{\cdot}9H_2O$ crystal structure

Water #	Wannier dipole moments in an ion-free $Al(NO_3)_3{\cdot}9H_2O$ crystal structure
W1	0.73
W2	1.72
W3	1.58
W4	1.14
W5	1.60
W6	1.73
W7	3.13
W8	2.48
W9	2.62

Influence of the "external" electric field. Fig. 5 showed that the dipole moment *vs.* H-bond donated O···O distance correlation is clearly strong in $Al(NO_3)_3{\cdot}9H_2O$. One may nevertheless question how well only the nearest environment on one side of the water molecule represents the influence from the full surroundings. In the previous paragraph we discussed the relative roles of ions and water neighbours. Next we will use the electric field – created by all the ions and water neighbours – over the whole water molecule as the measure.

Bogatko *et al.*[12] did not use the electric field but rather the electrostatic potential. For aqueous solutions of Ca^{2+}, Zn^{2+}, Fe^{3+} and Al^{3+}, they correlated the calculated water dipole moment and also the O···O distance between the first and second hydration shells with Z_{ion}/R_{ion}, a quantity they term "the charge density". They found, perhaps as expected, that the dipole moment increases and that the O···O distance decreases with increasing Z_{ion}/R_{ion} value. We think it may be even more illuminating to examine the dipole moment variation with respect to the external electric field.

Bucher and Kuyucak[2] did that for the water molecules in $M^{q+}(H_2O)_n$ clusters with $M^{q+} = K^+$ or Ca^{2+} and $n = 1,\ldots, 6$. They calculated the Wannier dipole moments for the water molecules in these clusters and evaluated the electric field at the oxygen position in the water molecules using a type of electrostatically derived charges. Setting $\mu^0 = 1.86$ D for the isolated-water dipole moment and $\alpha = 1.45$ Å^3 (9.79 a.u.) for the water molecule polarizability, they found that the equation $\mu = \mu^0 + \alpha{\cdot}E$ described the relation between the electric field strengths (E) and their calculated Wannier dipole moments in an excellent way. Thus they found a linear dependence in their calculated electric field range 0–5 V Å^{-1} (0–0.10 a.u.) and dipole moment range 1.86–4.2 D. This is in contrast to our results which suggest a non-linear 'dipole moment *vs.* electric field' behavior in the same field range (with our mode of calculating fields).

For $Al(NO_3)_3{\cdot}9H_2O$ we proceeded as follows. For each water molecule, the electric field generated by the other water molecules and ions in the crystal ("the external electric field") was calculated at both the O and H sites since quantum-mechanical calculations for the isolated water molecule in small uniform electric fields[36] suggested that the dipole polarizabilities of both the O and the H atoms are appreciable. In our study, the anisotropic electric field over each water molecule was calculated from a summation over an infinite periodic array of point charges with the help of the GULP program.[37] Only the field component along the water bisector was calculated since (i) we found above that the total – and thus induced – water dipole moment is almost collinear with the water bisector, and (ii) it was shown in ref. 36 that only the field component along the bisector has any appreciable influence on the polarization along the bisector. Several sets of charges (*e.g.* Wannier positions and charges, Bader charges) were tested in the field calculations.

The green circles in Fig. 6 display the Wannier dipole moments of the nine water molecules as a function of the external electric field (E), calculated for each molecule in turn as the field generated by the Wannier center and the nuclei of

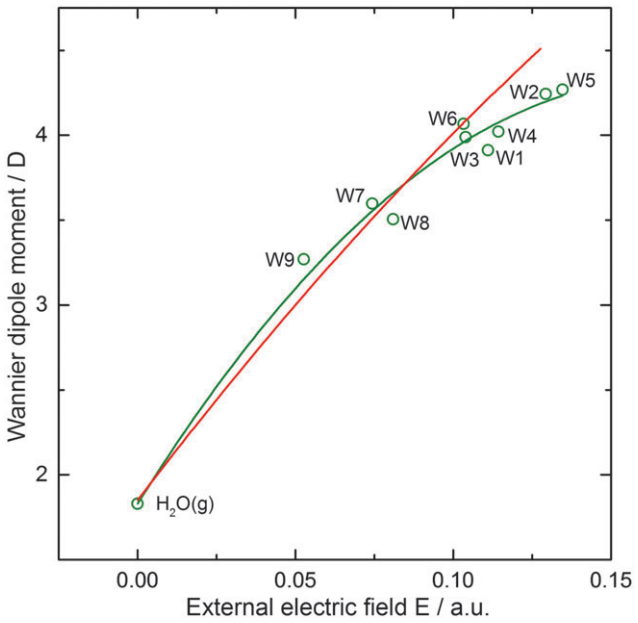

Fig. 6 The calculated Wannier dipole moment *vs.* external electric field strength for the nine water molecules in $Al(NO_3)_3{\cdot}9H_2O$(s) and for H_2O(g) (green circles). The electric field strengths E are mean values of the electric fields at the positions of O, H1 and H2 in the direction of the H1–O–H2 angle bisector. The green line is the least-squares fitted equation $\mu = \mu^0 + \alpha{\cdot}E + 1/2{\cdot}\beta{\cdot}E^2$ where the dipole moment for H_2O(g) μ^0 = 1.83 D, the polarizability α = 11.7 a.u. and the first dipole hyperpolarizability β = −69.8 a.u. The red line is drawn for the corresponding *experimental values* μ^0 = 1.85 D,[1] α = 9.6 a.u.[38] and β = −22 a.u.[39]

all the molecules and ions *outside* the probed water molecule and given as the *mean value* of the electric field strengths at the oxygen atom and the two hydrogen atoms of the probed molecule, in the direction of its H–O–H angle bisector. We note that the calculated 'μ *vs.* E' relation is not linear. A least-squares fit of the expression (Model 1) $\mu = \mu^0 + \alpha{\cdot}E + 1/2{\cdot}\beta{\cdot}E^2$ to our calculated dipole moments was performed, where μ^0 represents the permanent dipole moment of the water molecule, α the dipole polarizability, and β the first dipole hyperpolarizability of a water molecule. We constrained the curve to go through μ^0 = 1.83 D which is our VASP-calculated value for the isolated water molecule. The result is α = 11.7 a.u. and β = −69.8 a.u. (green line). The red line shows the function $\mu = \mu^0 + \alpha{\cdot}E + 1/2{\cdot}\beta{\cdot}E^2$, using experimental values for the permanent dipole moment, the dipole polarizability and the first dipole hyperpolarizability, namely μ^0 = 1.85 D,[1] α = 9.6 a.u.[38] and β = −22 a.u..[39] Our points are seen to lie below the "experimental" curve at high electric field. Clearly the local electric fields in the $Al(NO_3)_3{\cdot}9H_2O$ crystal represent very high field strengths. It is also worth pointing out that there are many simplifications in our approach: the chosen recipe to take the average of the electric field strengths at three selected probe points, the chosen point charges that create the field, and the truncation of the dipole moment expansion after the first dipole hyperpolarizability, to name a few.

In the following we show results from calculations where we treated each atom in the water molecule as a polarizable entity. Two models were explored, both involving atomic polarizabilities (α), but without or with dipole hyperpolarizabilities (β) added. In the former case, the model expression (Model 2) was "$\mu_{molecule} = \mu^0_{molecule} + \alpha_O{\cdot}E(\text{at O}) + \alpha_H{\cdot}E(\text{at H1}) + \alpha_H{\cdot}E(\text{at H2})$", which was fitted to the nine calculated molecular Wannier dipole moments. In this expression, the "external" electric field strengths at each nucleus were calculated using the GULP program as described above. A scatter plot of $\mu^{Wannier}_{molecule}$ *vs.* $\mu^{model}_{molecule}$ (not reproduced here) showed that the fit was good and of about the same quality as that for the molecular model, *i.e.* Model 1 (that scatter plot is not shown for that one either). The fitted α_O was almost three times that of α_H, which happens to be in good agreement with the relative magnitudes found by Krijn and Feil.[36] The sum $\alpha_O + 2\alpha_H$ becomes 8.3 a.u. in our calculations.

The expression for Model 3 also includes β_O and β_H and the squared electric field strengths at each nucleus. Four variables (α_O, α_H, β_O, β_H) were fitted against the nine "observations", *i.e.* the nine Wannier water dipole moments. The quality of the fit was very good, with all deviations smaller than 0.1 D, actually generally much smaller. Here α_H and α_O became similar in magnitude and $\alpha_O + 2\alpha_H$ was 11.4 a.u. Based on the quality of the fit it is not obvious which model to favour (and we have not made any statistical significance test), but it is clear that the Wannier data points in Fig. 6 suggest a non-linear polarization behavior for the extremely large external fields that perturb the W1–W6 water molecules in this crystal (a field of 0.10 a.u., for example, is 5.1×10^{10} V m^{-1}).

Relaxation of the internal geometry decreases the dipole moment. It is common to ascribe the polarization of a water molecule in condensed matter (compared to an isolated water molecule) both to the change in internal geometry and to electronic polarization effects. For the $Al(NO_3)_3{\cdot}9H_2O$ crystal, we find that the water dipole moment increases by 1.4–2.4 D (Wannier) and 0.7–1.5 D (Bader) when the isolated molecule is embedded in the crystal. Almost all of this polarization originates from electronic effects, and only a small part is the result of the different geometries that the molecules adopt in the crystal. This can be seen in Table 4. Here we have fixed the geometry of *an isolated water molecule* at the (nine) different geometries that the water molecules adopt in the

Table 4 Wannier dipole moments of isolated water molecules fixed at the geometry of the respective water molecule in the $Al(NO_3)_3{\cdot}9H_2O$ crystal; the first value pertaining to the calculated structure and the value in parentheses pertaining to the experimental structure from ref. 15

Water #	Wannier dipole moment in crystal geometry
W1	1.71 (1.72)
W2	1.79 (1.79)
W3	1.71 (1.72)
W4	1.74 (1.74)
W5	1.78 (1.79)
W6	1.79 (1.79)
W7	1.81 (1.82)
W8	1.79 (1.80)
W9	1.81 (1.80)

crystal and calculated the dipole moment using the Wannier analysis. The variation of the dipole moment is small, less than 0.1 D, and the resulting value is always smaller than the isolated-water dipole moment. This (small) decrease turns out to mostly be an effect of the opening of the H–O–H angle in the crystal (Table S2, ESI†) compared to the isolated molecule, and the dipole moment correlates very well with the projection along the water molecule bisector of the average O–H bond lengths for each water molecule (no graph shown here).

Although the effect of the internal geometry on the dipole moment appears to be modest, we saw in Fig. 4 that the correlation between the water dipole moment in the crystal and the average O–H distance within each molecule in the crystal is quite good. This is not a result of the effect of the internal geometry on the dipole moment (see the previous paragraph), but a consequence of the fact that both these properties are affected by the polarizing field from the long- and short-range crystalline environment surrounding the water molecules (what we call "the external field").

3.4 Electron distribution

The difference electron density, $\Delta\rho$, defined in the Method section, is displayed in the planes of all water molecules in Fig. 7. The reference state for each water is the isolated molecule with the same geometry as in the optimized crystal.

The nine water molecules all show the same *qualitative* pattern of electron displacement, namely in the direction from the hydrogen atoms towards the oxygen atom and beyond, reflecting an enhanced induced dipole moment along the water bisector. This is more pronounced for W1,..., W6 than for W7, W8 and W9. In the difference density maps, this is seen as electron depletions (dashed contour lines) close to the hydrogen nuclei and in the lone pair regions of the oxygen atoms. Electron excess (solid contour lines) is found close to the oxygen nuclei in the region of the O–H covalent bonds and

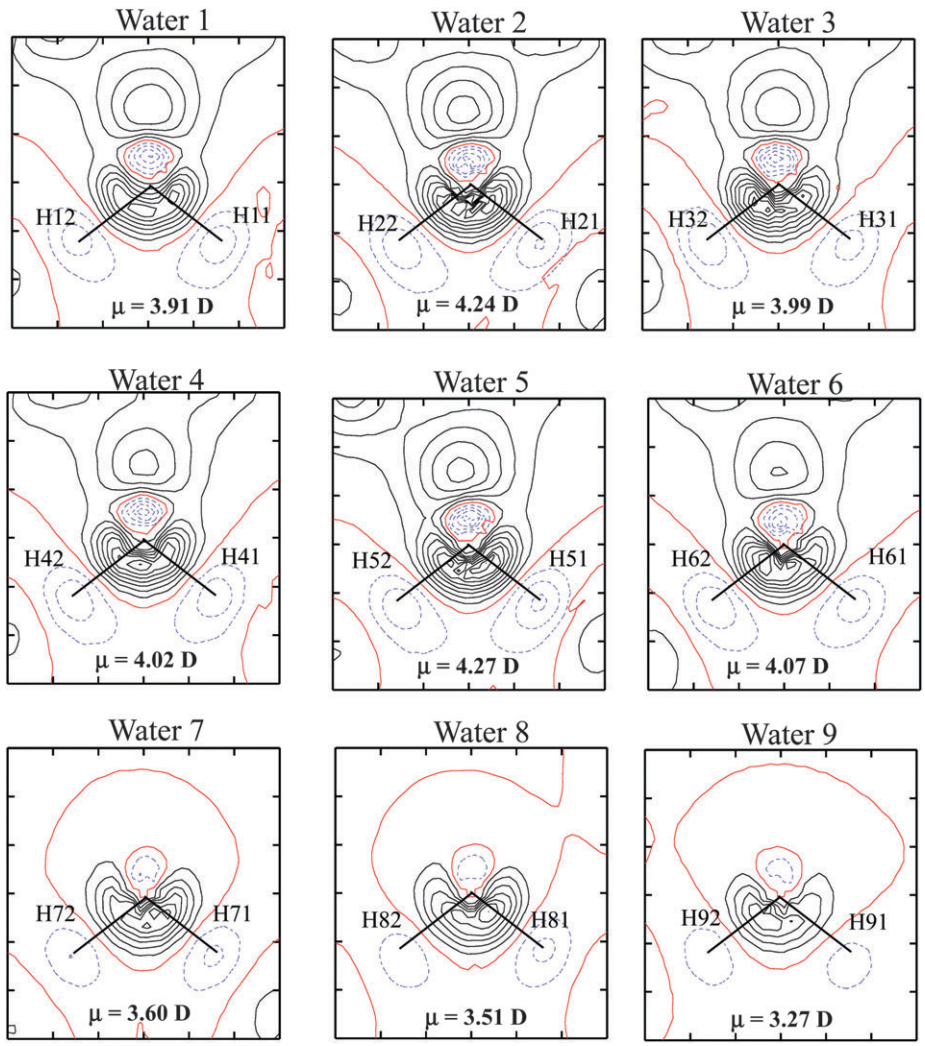

Fig. 7 Calculated difference electron densities in the plane of the nine water molecules in $Al(NO_3)_3{\cdot}9H_2O$(s). Solid lines are for positive and dashed lines for negative difference densities. The red solid line is the zero level. The contour interval is 0.05 e Å^{-3}. The values of water dipole moments are from the Wannier analysis.

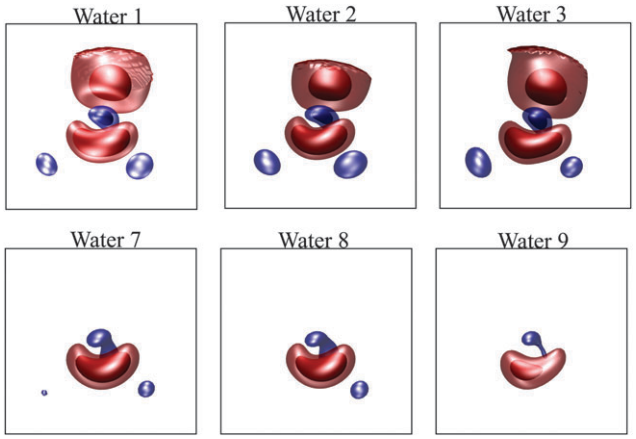

Fig. 8 Calculated difference electron densities for the water molecules W1, W2, W3, W7, W8 and W9 in $Al(NO_3)_3{\cdot}9H_2O$(s) shown as isosurface diagrams. Blue surfaces at −0.10 and −0.20 e Å^{-3}, red surfaces at +0.10 and +0.20 e Å^{-3}. The corresponding diagrams for W4, W5 and W6 show features very similar to those for W1, W2 and W3.

Table 5 Atomic charges (*e*) from a Bader analysis of the optimized crystal structure. The numbering of molecules and atoms follows ref. 15 and is consistent with Fig. 1. Both the aluminium ions have the charge +2.52 *e*

	Water molecules			
	O	H1	H2	Total
W1	−1.32	+0.64	+0.64	−0.04
W2	−1.32	+0.64	+0.64	−0.04
W3	−1.32	+0.64	+0.65	−0.03
W4	−1.32	+0.64	+0.64	−0.04
W5	−1.33	+0.64	+0.64	−0.05
W6	−1.31	+0.64	+0.64	−0.03
W7	−1.21	+0.62	+0.62	+0.03
W8	−1.20	+0.63	+0.62	+0.05
W9	−1.19	+0.61	+0.61	+0.03

	Nitrate ions				
	N	O1	O2	O3	Total
NO_3^-(1)	+0.83	−0.51	−0.53	−0.58	−0.79
NO_3^-(2)	+0.84	−0.54	−0.54	−0.55	−0.79
NO_3^-(3)	+0.84	−0.58	−0.51	−0.55	−0.80

for W1,..., W6 also in the direction of the aluminium ions. For water molecules W7, W8 and W9, the corresponding electron excess in the hydrogen bond-accepting directions is much smaller.

The larger electron redistributions seen for W1,..., W6 are consistent with their shorter hydrogen bonds and larger molecular dipole moments compared to W7, W8 and W9. In some of the water molecules, the electron excess is clearly asymmetrically distributed in the two covalent O–H bonds. In these cases the larger electron density maximum is associated with the stronger hydrogen bond. For example, the O3–H32···O7 hydrogen bond is stronger (shorter) than the O3–H31···O33 hydrogen bond.

Fig. 8 shows a 3-dimensional isosurface representation of $\Delta\rho$ for six representative water molecules and their surroundings.

3.5 Atomic charges – from clusters to crystals

The atomic charges for the optimized crystal are given in Table 5. These are Bader-type charges, *i.e.* integrated over the atomic Bader volumes. We note that the net charges of the water molecules fall into two groups: the slightly negative ones (W1,..., W6) and the slightly positive ones (W7, W8 and W9). All the 18 H atoms have very similar charges (between +0.61 and +0.64 *e*) while the variation for the O atoms is larger (between −1.19 and −1.33 *e*) with the most negative values for the O atoms directly bonded to an aluminium ion. The two crystallographically non-equivalent aluminium ions display very similar charges and so do the three nitrate ions.

For each of the nine water molecules in $Al(NO_3)_3{\cdot}9H_2O$(s), the magnitude of the net Bader charge is 0.05 *e* or less. This is seemingly in contrast to some results for hydrated cations in the literature, where the calculated water charges have been reported to be considerably larger. For example, molecular DFT calculations (B3LYP/6-311+G(2d,2p)//B3LYP/LANL2DZ) performed by Pavlov *et al.*[40] showed net water charges of +0.47, +0.23, +0.18, +0.12, +0.07 and +0.07 *e* for $Be(H_2O)^{2+}$, $Be(H_2O)_6^{2+}$, $Mg(H_2O)^{2+}$, $Mg(H_2O)_6^{2+}$, $Ca(H_2O)^{2+}$ and $Ca(H_2O)_6^{2+}$, respectively. For the same complexes, Cappa *et al.*[41] also performed DFT-based molecular calculations (although of a different flavour than ref. 40) and found almost identical values as in ref. 40. In both these references the reported charges were of the Mulliken type in contrast to our Bader charges. The ion most similar to our Al^{3+} ion is Be^{2+}, whose charge-to-radius ratio is quite similar to that of Al^{3+} and also very large. Clearly, the net water charge reported for the $Be(H_2O)_6^{2+}$ complex (+0.23 *e*) in ref. 36 is much larger than our values for the first-shell water molecules in the $Al(NO_3)_3{\cdot}9H_2O$ crystal (−0.03 to −0.05 *e*).

We believe this discrepancy comes from two sources: the isolated clusters *vs.* the crystal, and the method to calculate the charges. To illuminate the situation we have performed calculations (PBE/6-311G**; see the Method section) on some Al^{3+} complexes taken out from the crystal with preserved optimized-crystal geometry. We have chosen W2 as a representative water molecule, so that all complexes contain the W2 molecule and the Al1 ion. In Fig. 9 we follow how the surroundings of Al1, and especially W2, are built up, starting from Al–W2 (cluster **A**), and proceeding to cluster **E**. We have selected the cluster charges in a consistent manner, such that the net charges of clusters **A**, **B**, **C**, **D** and **E** are 3+, 3+, 2+, 2+ and 0 *e*, respectively. Four types of charges available from, or in connection with, the Gaussian program were calculated, namely Mulliken charges, Bader charges, electrostatic potential-derived charges of the Chelpg type, and NBO (Natural Bond Orbital analysis-derived) charges. The resulting charges for all constituent molecules/ions are listed in Table S4 (ESI†).

Fig. 10 visualizes the results, for Al1 in Fig. 10(a) and for the net W2 charge in Fig. 10(b). We conclude the following.

(i) For all investigated cases, the Mulliken charges display much larger electron transfer from the water molecules to the cation than the other methods do, especially compared to the Bader charges. Consequently, the Al charge becomes small and

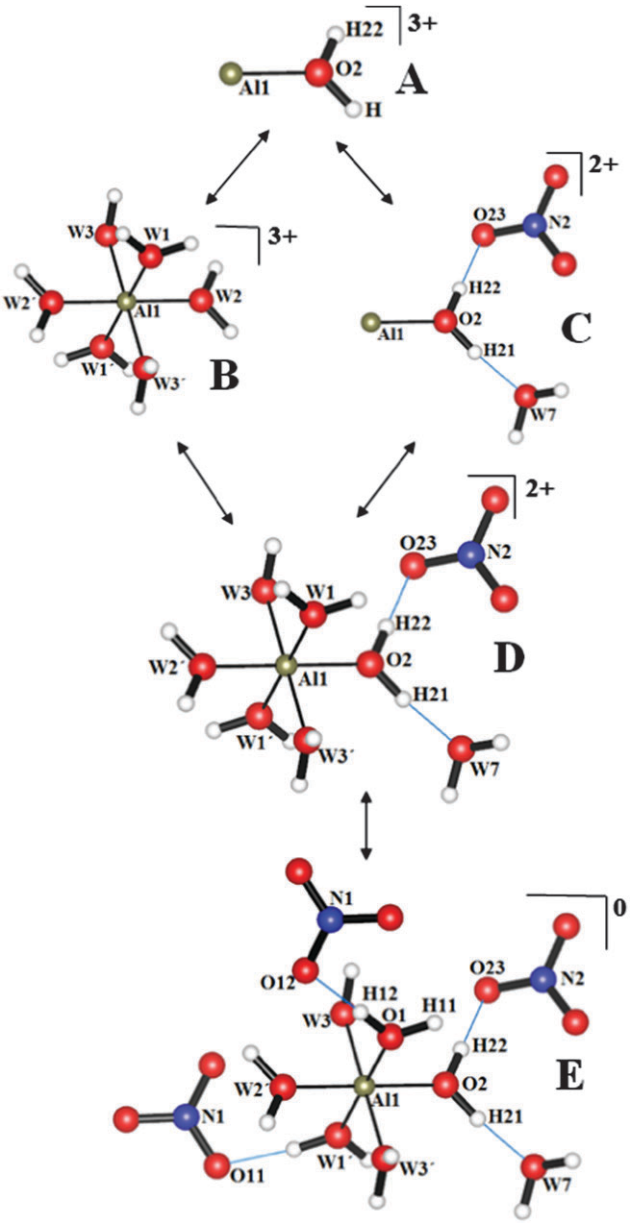

Fig. 9 Five complexes (**A**, **B**, **C**, **D** and **E**) taken out from the $Al(NO_3)_3 \cdot 9H_2O$ calculated crystal structure with preserved geometry.

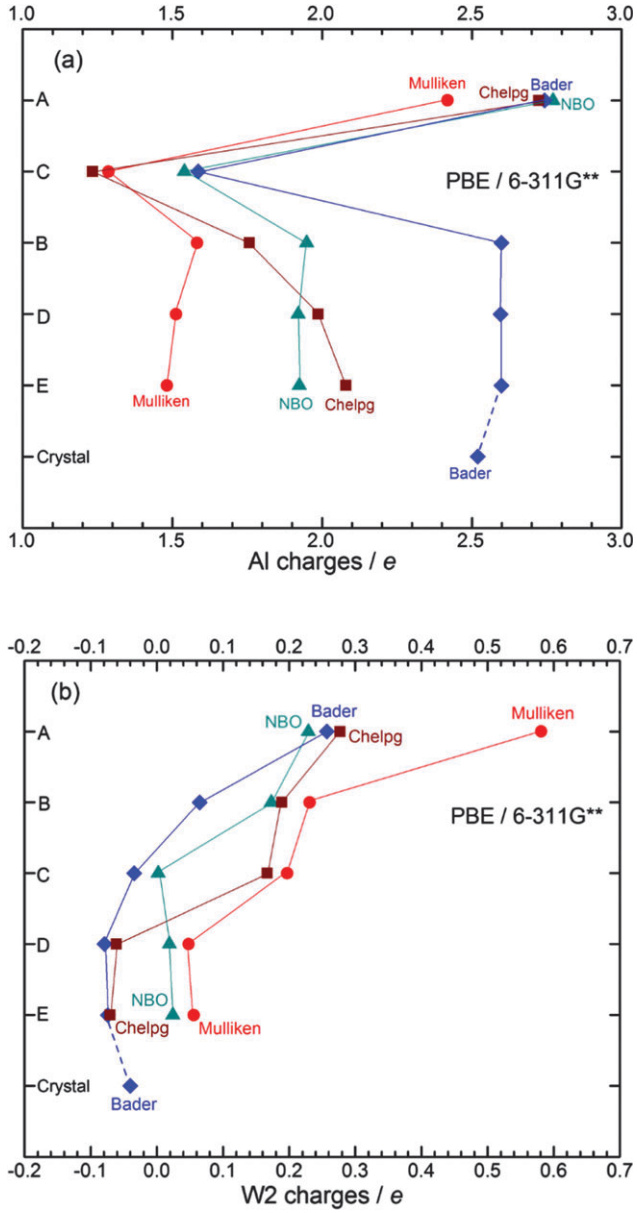

Fig. 10 Charges of various types calculated for the complexes **A**, **B**, **C**, **D** and **E** as displayed in Fig. 9. (a) The charges of the Al1 atom and (b) the charges of the W2 water molecule. Note that the order of the complexes on the vertical scale is not the same for (a) and (b).

the W2 charge large with the Mulliken method and less so with the Bader method. The other methods lie in between.

(ii) All the four types of charges displayed in Fig. 10 show the same trends with respect to cluster size increase.

(iii) When going from complex **A** to complex **E**, the charge on Al (Fig. 10(a)) has stabilized already for complex **B** and the W2 charge (Fig. 10(b)) has stablilized already for complex **D**. In both cases, these are the clusters where all the nearest neighbours are present.

(iv) Using all methods (even with the Mulliken approach), the magnitude of the W2 charge in complex **E** is less than 0.06 *e*. This is small and consistent with the Bader charge we obtained for the $Al(NO_3)_3 \cdot 9H_2O$ crystal (the line between cluster **E** and the crystal is dashed to highlight that the electronic structure methods used for the crystal and the clusters, PBE/(PAW + plane-wave basis) and PBE/6-311G**, are not identical).

4. Concluding remarks

$Al(NO_3)_3 \cdot 9H_2O$ serves as a "benchmark compound" for H-bond relations and water binding, since it contains so many water molecules representing a range of different bonding situations. The main conclusions to draw from the present quantum-mechanical calculations are as follows.

• The many correlation curves that have been published in the literature for H-bond properties, such as H···O *vs.* O···O

distance correlations, are almost always based on data for different crystals and from different experiments. Here we explore such correlations within the $Al(NO_3)_3{\cdot}9H_2O$ compound since the H-bond network in this crystal spans large H···O and O···O distance ranges. We find good correlations (Fig. 2 and 3) and in fact a more sensible O–H *vs.* H···O distance correlation than experimental neutron diffraction data are able to yield.

• The dipole moment of the water molecule increases by 80–135% due to its surroundings in the crystal. There are two clear categories: the first-shell water molecules around Al^{3+} and the others (Table 2).

• The Bader dipole moment lies about 1 D below the Wannier dipole moment for all water molecules in the crystal (for the gas-phase water molecule the difference is, and should be, zero) (Fig. 4).

• The water dipole moments in the crystal are found to correlate very well with the mean O···O distance of their donated hydrogen bonds (Fig. 5). Literature data from CPMD simulations for ionic aqueous solutions were compared with our crystalline results and were found to adhere quite well to the same correlation curve.

• The nine Wannier type water dipole moments also correlate well with the external electric field over the molecule (*i.e.* the field created from all the neighbours outside the probed molecule (Fig. 6)). Three different models were explored: molecular (hyper)polarizabilities, atomic polarizabilities, or atomic polarizabilities plus atomic dipole hyperpolarizabilities. A fit of the variables in the second model, $\mu_{molecule} = \mu^0_{molecule} + \alpha_O{\cdot}E(\text{at O}) + \alpha_H{\cdot}E(\text{at H1}) + \alpha_H{\cdot}E(\text{at H2})$, against the molecular Wannier dipole moments gives an α_O value almost three times that of α_H.

• The details of the difference electron density maps (Fig. 7 and 8) reveal significant differences between the two main categories of water molecules, and strong similarities of the features within these groups.

• The progression of the water and cation charges from '*small clusters* ⇒ *large clusters* ⇒ *the crystal*' (Fig. 10) helps explain why the net charges on all the water molecules are so small in the crystal.

Acknowledgements

This work is supported by the Swedish Research Council (VR) and the Swedish national Strategic e-Science program eSSENCE. The simulations were performed on resources provided by the Swedish National Infrastructure for Computing (SNIC) at UPPMAX and NSC. IB thanks Uppsala University for hospitality during research visits and Hungarian OTKA grant number K108721.

References

1 S. A. Clough, Y. Beers, G. P. Klein and L. S. Rothman, *J. Chem. Phys.*, 1973, **59**, 2254.
2 D. Bucher and S. Kuyucak, *J. Phys. Chem. B*, 2008, **112**, 10786.
3 D. Marx, M. Sprik and M. Parrinello, *Chem. Phys. Lett.*, 1997, **273**, 360.
4 F. C. Lightstone, E. Schwegler, R. Q. Hood, F. Gygi and G. Galli, *Chem. Phys. Lett.*, 2001, **343**, 549.
5 I. Bako, J. Hutter and G. Palinkas, *J. Chem. Phys.*, 2002, **117**, 9838.
6 T. Ikeda, M. Hirata and T. Kimura, *J. Chem. Phys.*, 2003, **119**, 12386.
7 T. Ikeda, M. Hirata and T. Kimura, *J. Chem. Phys.*, 2005, **122**, 0245101.
8 T. Ikeda, M. Hirata and T. Kimura, *J. Chem. Phys.*, 2005, **122**, 2445071.
9 T. Ikeda, M. Boero and K. Terakura, *J. Chem. Phys.*, 2007, **126**, 0345011.
10 T. Ikeda, M. Boero and K. Terakura, *J. Chem. Phys.*, 2007, **127**, 0745031.
11 E. Bylaska, M. Valiev, J. R. Rustad and J. H. Weare, *J. Chem. Phys.*, 2007, **126**, 104505.
12 S. Bogatko, E. Cauët, E. Bylaska, G. Schenter, J. Fulton and J. Weare, *Chem. – Eur. J.*, 2013, **19**, 3047.
13 C. Krekeler and L. Delle Site, *J. Phys.: Condens. Matter*, 2007, **19**, 1921011.
14 T. W. Whitfield, S. Varma, E. Harder, G. Lamoureux, S. B. Rempe and B. Roux, *J. Chem. Theory Comput.*, 2007, **3**, 2068.
15 K. Hermansson, *Acta Crystallogr., Sect. C: Cryst. Struct. Commun.*, 1983, **39**, 925.
16 J. P. Perdew, K. Burke and M. Ernzerhof, *Phys. Rev. Lett.*, 1996, **77**, 3865.
17 S. Grimme, *J. Comput. Chem.*, 2006, **27**, 1787.
18 P. E. Blöchl, *Phys. Rev. B: Condens. Matter Mater. Phys.*, 1994, **50**, 17953.
19 H. J. Monkhorst and J. D. Pack, *Phys. Rev. B: Solid State*, 1976, **13**, 5188.
20 G. Kresse and J. Furthmüller, *Phys. Rev. B: Condens. Matter Mater. Phys.*, 1996, **54**, 11169.
21 G. Kresse and J. Hafner, *Phys. Rev. B: Condens. Matter Mater. Phys.*, 1993, **47**, 558.
22 R. F. W. Bader and C. F. Matta, *J. Phys. Chem. A*, 2004, **108**, 8385.
23 R. F. W. Bader, *Atoms in Molecules – A Quantum Theory*, Oxford University Press, 1990.
24 G. Henkelman, A. Arnaldsson and H. Jonsson, *Comput. Mater. Sci.*, 2006, **36**, 354.
25 N. Marzari and D. Vanderbilt, *Phys. Rev. B: Condens. Matter Mater. Phys.*, 1997, **56**, 12847.
26 A. A. Mostofi, J. R. Yates, Y.-S. Lee, I. Souza, D. Vanderbilt and N. Marzari, *Comput. Phys. Commun.*, 2008, **178**, 685.
27 R. Krishnan, J. S. Binkley, R. Seeger and J. A. Pople, *J. Chem. Phys.*, 1980, **72**, 650.
28 M. J. Frisch, G. W. Trucks, H. B. Schlegel, G. E. Scuseria, M. A. Robb, J. R. Cheeseman, G. Scalmani, V. Barone, B. Mennucci, G. A. Petersson, H. Nakatsuji, M. Caricato, X. Li, H. P. Hratchian, A. F. Izmaylov, J. Bloino, G. Zheng, J. L. Sonnenberg, M. Hada, M. Ehara, K. Toyota, R. Fukuda, J. Hasegawa, M. Ishida, T. Nakajima, Y. Honda, O. Kitao,

H. Nakai, T. Vreven, J. A. Montgomery Jr, J. E. Peralta, F. Ogliaro, M. Bearpark, J. J. Heyd, E. Brothers, K. N. Kudin, V. N. Staroverov, R. Kobayashi, J. Normand, K. Raghavachari, A. Rendell, J. C. Burant, S. S. Iyengar, J. Tomasi, M. Cossi, N. Rega, N. J. Millam, M. Klene, J. E. Knox, J. B. Cross, V. Bakken, C. Adamo, J. Jaramillo, R. Gomperts, R. E. Stratmann, O. Yazyev, A. J. Austin, R. Cammi, C. Pomelli, J. W. Ochterski, R. L. Martin, K. Morokuma, V. G. Zakrzewski, G. A. Voth, P. Salvador, J. J. Dannenberg, S. Dapprich, A. D. Daniels, Ö. Farkas, J. B. Foresman, J. V. Ortiz, J. Cioslowski and D. J. Fox, *J. Gaussian, 09, Revision A.02*, Gaussian Inc., Wallingford, CT, 2009.

29 D. Lazar, B. Ribár and B. Prelesnik, *Acta Crystallogr., Sect. C: Cryst. Struct. Commun.*, 1991, **47**, 2282.

30 G. V. Yukhnevich, *Crystallogr. Rep.*, 2009, **54**, 184.

31 R. L. Cook, F. C. De Lucia and P. Helminger, *J. Mol. Spectrosc.*, 1974, **53**, 62.

32 A. Eriksson, K. Hermansson, J. Lindgren and J. O. Thomas, *Acta Crystallogr., Sect. A: Cryst. Phys., Diffr., Theor. Gen. Crystallogr.*, 1982, **38**, 138.

33 A. Eriksson, B. Berglund, J. Tegenfeldt and J. Lindgren, *J. Mol. Struct.*, 1979, **52**, 107.

34 A. K. Soper and C. J. Benmore, *Phys. Rev. Lett.*, 2008, **101**, 0655021.

35 P. J. Dyer and P. T. Cummings, *J. Chem. Phys.*, 2006, **125**, 1445191.

36 M. P. C. M. Krijn and D. Feil, *J. Phys. Chem.*, 1987, **91**, 540.

37 J. D. Gale, *J. Chem. Soc., Faraday Trans.*, 1997, **93**, 629.

38 G. D. Zeiss, W. R. Scott, N. Suzuki, D. P. Chong and S. R. Langhoff, *Mol. Phys.*, 1979, **37**, 1543.

39 J. F. Ward and C. K. Miller, *Phys. Rev. A: At., Mol., Opt. Phys.*, 1979, **19**, 826.

40 M. Pavlov, P. E. M. Siegbahn and M. Sandström, *J. Phys. Chem. A*, 1998, **102**, 219.

41 C. D. Cappa, J. D. Smith, B. M. Messer, R. C. Cohen and R. J. Saykally, *J. Phys. Chem. B*, 2006, **110**, 5301.